

May 2013

carlomat, version 2
**of the program for automatic computation of lowest
order cross sections**

Karol Kołodziej¹

*Institute of Physics, University of Silesia
ul. Uniwersytecka 4, PL-40007 Katowice, Poland*

Abstract

Version 2 of carlomat, a program for automatic computation of the lowest order cross sections of multiparticle reactions, is described. The substantial modifications with respect to version 1 of the program include: generation of a single phase space parametrization for the Feynman diagrams of the same topology, an interface to parton density functions, improvement of the color matrix computation, the Cabibbo-Kobayashi-Maskawa mixing in the quark sector, the effective models including scalar electrodynamics, the Wtb interaction with operators of dimension up to 5 and a general top-higgs coupling. Moreover, some minor modifications have been made and several bugs in the program have been corrected.

¹E-mail: karol.kolodziej@us.edu.pl

PROGRAM SUMMARY

Program title: carlomat, version 2.0

Catalogue identifier:

Program summary:

Program obtainable from: CPC Program Library, Queen's University, Belfast, N. Ireland

Licensing provisions: Standard CPC licence

No. of lines in distributed program, including test data, etc.:

No. of bytes in distributed program, including test data, etc.:

Distribution format: tar.gz

Programming language: Fortran 90/95

Computer: all

Operating system: Linux

Classification:

Nature of problem: Leading order predictions for reactions of two particle scattering into a final state with up to 10 particles within the Standard Model and some effective models.

Solution method: A few substantial modifications are introduced with respect to version 1.0 of the program. First, a single phase space parametrization is generated for the Feynman diagrams of the same topology taking into account possible differences in mappings of peaks in the individual diagrams, which speeds up a compilation time of the Monte Carlo program for multiparticle reactions by a factor 4–5 with respect to the previous version. Second, an interface to parton density functions is added that allows to make predictions for hadron collisions. Third, the color matrix is divided into smaller routines and written down as a stand alone program that is calculated prior to compilation and execution of the Monte Carlo program for computation of the cross section. Fourth, the Cabibbo-Kobayashi-Maskawa mixing in the quark sector is implemented. Fifth, the effective models including scalar electrodynamics, the Wtb interaction with operators of dimension up to 5 and a general top-higgs coupling are implemented. Moreover, some minor modifications have been made and several bugs in the program have been corrected.

Restrictions: Although a compilation time has been shortened in the current version, it still may be quite long for processes with 8 or more final state particles, in particular those with the large size color matrix.

Running time: Depends strongly on the selected process and, to less extent, on the Fortran compiler used. The following amounts of time are needed at different computation stages that are performed to produce the appended test output files for the reaction $gg \rightarrow b\bar{u}\bar{d}\bar{b}\mu^-\bar{\nu}_\mu$, relevant for the top quark pair production, on a PC with the Pentium 4 3.0 GHz processor with, respectively, Absoft (GNU, Intel) Fortran compilers: code generation takes 3.7 s (3.7 s, 2.4 s) time, compilation, computation and simplification of the color matrix takes about 1 s (1 s, 1 s) time, compilation of all the generated routines takes just a few seconds and execution of the MC program takes about 44 s (41 s, 23 s) time.

LONG WRITE-UP

1 Introduction

In the era of the LHC reactions of production of a few heavy particles at a time, as, e.g., the electroweak gauge bosons, top quark or recently discovered scalar candidate for the higgs boson, have become commonplace. The heavy particles live so shortly that they should be actually regarded as the intermediate states of reactions with multiple light particles in the final state. As an example consider the following reactions

$$gg \rightarrow bud\bar{b}\mu^-\bar{\nu}_\mu, \quad (1)$$

$$u\bar{u} \rightarrow bud\bar{b}\mu^-\bar{\nu}_\mu, \quad (2)$$

which are underlying partonic processes of $pp \rightarrow t\bar{t}$, the top quark pair production in the proton-proton collisions at the LHC. The final state of (1) and (2) corresponds to each of the top quarks decaying into a b -quark and a W -boson and, subsequently one of the W bosons decaying leptonically and the other hadronically, as depicted in Figs. 1a, 1b, 2a and 2b. However, both reactions receive contributions from many other Feynman diagrams which do not represent the signal of the top quark pair production. Some examples of such diagrams are depicted in Figs. 1c–1f for reaction (1) and in Figs. 2c–2d for reaction (2). The entire number of the leading order Feynman diagrams of reactions (1) and (2) in the unitary gauge of the standard model (SM), with the neglect of the higgs boson coupling to fermions lighter than the b -quark and of the Cabibbo-Kobayashi-Maskawa (CKM) mixing amounts to 421 and 718, respectively.

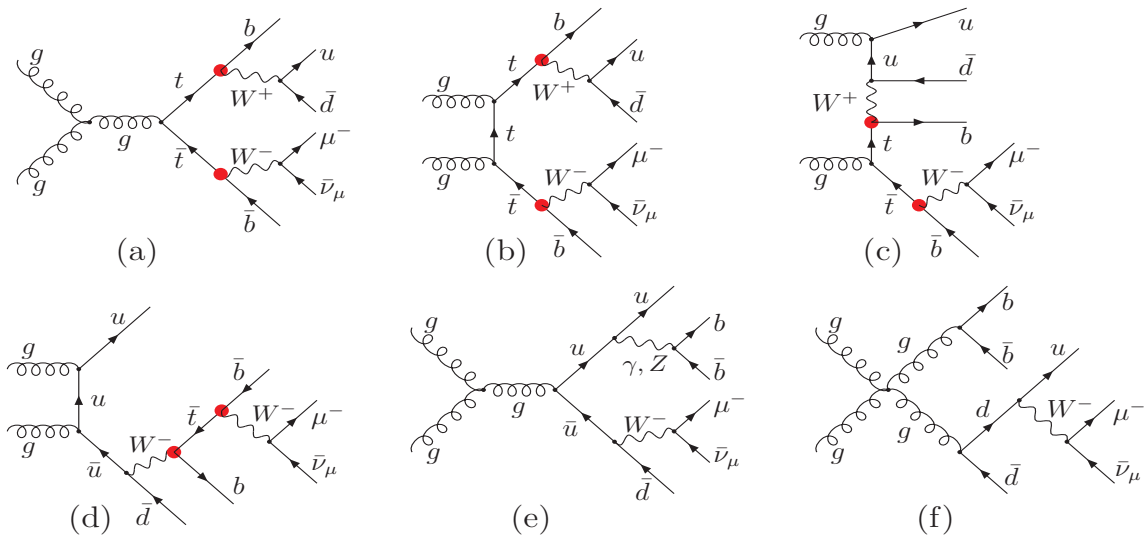


Figure 1: Examples of the leading order Feynman diagrams of process (1). Blobs indicate the Wtb coupling.

Another example is the reaction

$$gg \rightarrow bud\bar{b}\mu^-\bar{\nu}_\mu b\bar{b} \quad (3)$$

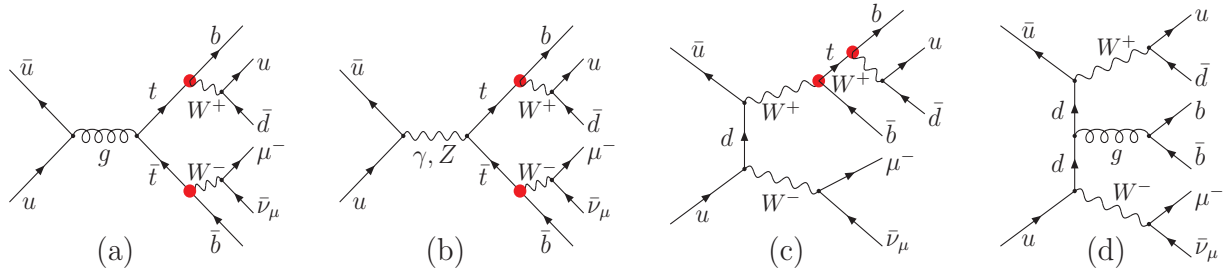


Figure 2: Examples of the leading order Feynman diagrams of process (2). Blobs indicate the Wtb coupling.

that is a dominant partonic process of the associated production of the top quark pair and higgs boson in the proton–proton collisions at the LHC, $pp \rightarrow t\bar{t}h$, where one of the top quarks decays hadronically, the other semileptonically and the higgs boson decays into the $b\bar{b}$ -pair, as depicted in Figs. 3a–3c. The diagrams depicted in Fig. 3d–3f are examples of the background contributions to associated production of the higgs boson and top quark pair. Under the same assumptions as above, the entire number of the Feynman diagrams is equal to 67 300.

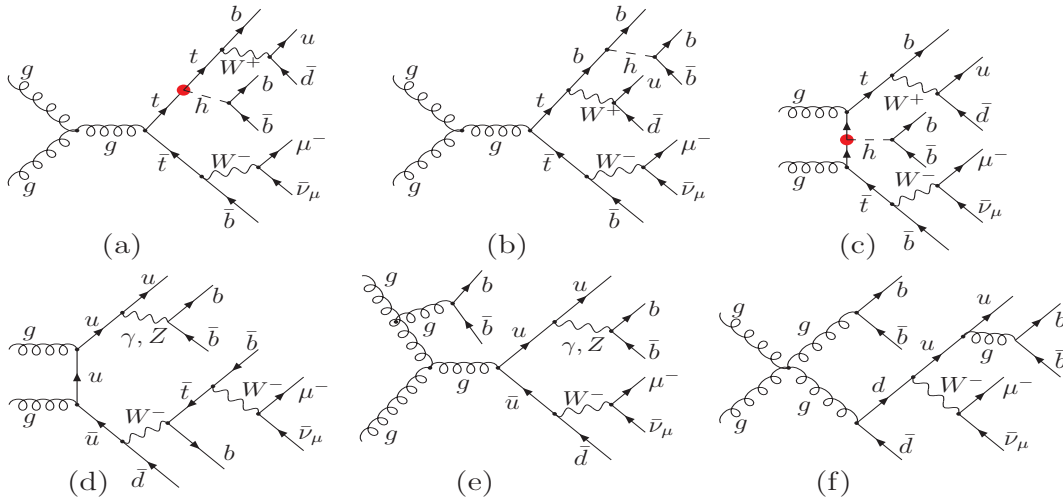


Figure 3: Examples of the lowest order Feynman diagrams of reaction (3): (a), (b) and (c) are the signal diagrams of $t\bar{t}h$ production, (d), (e) and (f) are the $t\bar{t}h$ background contributions. Blobs indicate the higgs–top coupling.

It is needless to say that reliable theoretical predictions for reactions as (1), (2) and (3) can be obtained only within a fully automated approach, as offered by, e.g., `carlomat` [1].

2 Basic changes in the program

In the following, the substantial changes in the program are described.

2.1 Phase space integration

The MC phase space integration in `carlomat` is performed with the use of multichannel approach. It is chosen because the number of peaks in the squared matrix element, that should be mapped out in order to improve convergence of the integral, usually by far exceeds the number of independent variables in a single parametrization of the phase space element given by Eqs. (17) and (19) of [1]. The peaks arise whenever the denominator of a propagator in any of the Feynman diagrams is approaching its minimum. In version 1 of the program, a separate phase space parametrization is generated for each Feynman diagram whose peaks are smoothed with appropriate mappings of the integration variables. A user specified number of individual phase space parametrizations are combined into a kinematical subroutine and then all the subroutines are combined into a single multichannel integration routine, as described in Sect. 2.4 of [1]. The number should be chosen so as to possibly minimize the compilation time which, however, is quite long for multiparticle processes with large number of the Feynman diagrams.

An improvement of the phase space integration in the current version of the program is based on a simple observation that the Feynman diagrams of the same topology differ from each other only in propagators of the internal particles. This means that the integration limits for all the variables of the phase parametrizations corresponding to those diagrams are the same and can be written down only once, commonly for all such parametrizations. The same holds for the Lorentz boosts of four momenta of the final state particles. The final state particles are divided in subsets that are characteristic for the topology. Their four momenta are randomly generated in the relative centre of mass frame of the subset and then boosted to the rest frame of the parent subset, and so on until they reach the centre of mass frame of all the final state particles.

In order to illustrate this procedure let us consider the diagram of reaction (3) depicted in Fig. 3a. The final state particles are divided in two subsets: $\{\{b, \bar{b}\}, \{b', \{u, \bar{d}\}\}\}$ and $\{\bar{b}', \{\mu^-, \bar{\nu}_\mu\}\}$, where a prime has been introduced in order to distinguish between the identical quarks in the diagram. The distinction makes sense, as there are 3 other dedicated phase space parametrizations for the diagrams that differ from the one in Fig. 3a by the exchanges: $b \leftrightarrow b'$ and/or $\bar{b} \leftrightarrow \bar{b}'$. Note, that the diagram of Fig. 3b, despite having the same shape as that of Fig. 3a, belongs to different topology in a sense described in Sect. 2.1 of [1]. Let us consider the subset $\{\{b, \bar{b}\}, \{b', \{u, \bar{d}\}\}\}$ first. The four momenta p_u and $p_{\bar{d}}$ are randomly generated in the frame, where $\vec{p}_u + \vec{p}_{\bar{d}} = \vec{0}$. The four momentum $p_{b'}$ is generated in the frame, where $\vec{p}_{b'} + \vec{p}_{\{u, \bar{d}\}} = \vec{0}$ and the four momenta p_u and $p_{\bar{d}}$ are boosted to this frame. The four momenta p_b and $p_{\bar{b}}$ are randomly generated in the frame, where $\vec{p}_b + \vec{p}_{\bar{b}} = \vec{0}$. Then $p_b, p_{\bar{b}}, p_{b'}, p_u$ and $p_{\bar{d}}$ are boosted to the frame, where $\vec{p}_{\{b, \bar{b}\}} + \vec{p}_{\{b', \{u, \bar{d}\}\}} = \vec{0}$. The four momenta of the second subset $\{\bar{b}', \{\mu^-, \bar{\nu}_\mu\}\}$ are generated analogously, but this time one Lorentz boost less is required. Finally, all the four momenta of final state particles are boosted to the centre of mass frame. Therefore the integration limits and calls to the boost subroutine are written commonly for all the phase space parametrizations corresponding to the Feynman diagrams of the same topology.

In the result of the modifications described above the phase space integration routine becomes shorter and a compilation time is substantially reduced compared to the previous version of the program, by a factor 4–5 for multiparticle reactions.

2.2 Hadron–hadron collisions

An interface to CTEQ6 [2] parton density functions is added in the MC computation part of the program. The user should choose if she/he wants to calculate the cross section of the hard scattering process at the fixed centre of mass energy, or to fold it with the parton density functions, treating the initial state particles as partons of either the $p\bar{p}$ or pp scattering. This is controlled by a single flag `ihad` in the main program of the MC computation `carlocom.f`. The program will automatically assign the integer labels to the initial state partons according to the convention of CTEQ6. The user should also choose which set of the CTEQ6 partons he wants to use by specifying the flag `iset`, with a recommended value `iset=3` that corresponds to the leading order partons and $\alpha_s(m_Z) = 0.118$. It is also possible to choose one of 3 predefined factorization scales Q by specifying a value of `iscl`: `iscl=1` ($Q=sclf*\sqrt{s'}$)/2 ($Q = sclf$)/3 ($Q=sclf*\sqrt{m_t^2+\text{sum of } p_{tj}^2}$), where `sclf` is an arbitrary real (double precision) value. The user can easily define other scales by changing the defining expressions for `qsc` in `croskk.f`.

In order to avoid a mismatch of parameters, the light quark masses and minimum value of Bjorken x are transferred from common blocks `XQrange` and `Masstbl` of CTEQ6 with a call to subroutine `ctq6f_interface.f` from `parfixkk.f`, where also a call to `SetCtq6(iset)`, that initializes the CTEQ6 parameters, is done. Because of the same reason, it is recommended to use the same value of $\alpha_s(m_Z)$ as is used in the corresponding set of parton distribution functions of CTEQ6. For user's convenience files `Ctq6Pdf.f` and `cteq6l.tbl` containing the parton distribution functions is included in the current distribution of `carlomat`.

2.3 Color matrix

The color matrix in `carlomat`, after its size being reduced with the help of some basic SU(3) algebra properties, is calculated numerically from the very definition, using explicit expressions for the SU(3) group structure constants and the Gell-Mann matrices. In version 1.0 of `carlomat`, the reduced color matrix was cast in a single subroutine `colsqkk.f` that was compiled together with all the other subroutines of the MC program and calculated anew every time the program was run. This posed no problem for processes with a simple color structure, but it unnecessarily increased the computation time for processes with a large size color matrix.

Compilation of the large subroutine containing the entire color matrix was very time consuming, therefore, in the current version of the program, a subroutine `colsqkk.f` is divided into smaller subroutines of the user controlled size which allows to compile much larger color matrices and speeds up the compilation process. Moreover, computation of the color matrix is performed as a separate stage, that is automatically executed just after the code generation. Then the resulting nonzero elements of the color matrix and their labels are transferred to the directory, where they are read by subroutine `mpo12.f` of the MC program when it is executed for the first time.

2.4 Cabibbo-Kobayashi-Maskawa mixing

The CKM mixing in the quark sector is implemented in the program. The CKM mixing would be an unnecessary complication for many applications, therefore, an option has been included in `carlomat.f` that allows to switch it on or off: `ickm=1(yes)/else(no)`.

For the sake of simplicity, only the magnitudes of the CKM matrix elements V_{ij} [3] are taken into account. However, as the W boson coupling to fermions, that always multiplies V_{ij} , is complex, complex phases of the CKM matrix can be easily incorporated. To do so, it is enough to change the type of V_{ij} in `inprms.f` to complex and make a distinction between the $Wf\bar{f}'$ couplings and their conjugates in `vertices.dat.ckm`. The latter is a new data file that must be present in directory `code_generation` together with `vertices.dat` that defines the couplings in absence of the CKM mixing.

If the CKM mixing is included then the numbers Feynman diagrams of reactions (1) and (2) in the unitary gauge of SM, with the neglect of the higgs boson coupling to fermions lighter than c -quark, increase to 596 and 1444, respectively.

2.5 Anomalous Wtb coupling

The top quark mass is close to the energy scale of the electroweak symmetry breaking. Therefore it is possible that the top quark coupling to the W -boson differs from the $V - A$ form of SM. The Wtb coupling is present in any process of the top quark production if a top quark decay in the dominant Wb channel is taken into account. Not only does it enter the signal Feynman diagrams of the top quark production and decay, but it is present also in many other diagrams which represent the off resonance background contributions to the top quark production. This is illustrated in Figs. 1 and 2, where the Wtb coupling is indicated by red blobs.

The effective Lagrangian of the Wtb interaction containing operators of dimension four and five that is implemented in the current version of the program has the following form [4]:

$$\begin{aligned}
 L_{Wtb} = & \frac{g}{\sqrt{2}} V_{tb} \left[W_{\mu}^{-} \bar{b} \gamma^{\mu} (f_1^L P_L + f_1^R P_R) t - \frac{1}{m_W} \partial_{\nu} W_{\mu}^{-} \bar{b} \sigma^{\mu\nu} (f_2^L P_L + f_2^R P_R) t \right] \\
 & + \frac{g}{\sqrt{2}} V_{tb}^{*} \left[W_{\mu}^{+} \bar{t} \gamma^{\mu} (\bar{f}_1^L P_L + \bar{f}_1^R P_R) b - \frac{1}{m_W} \partial_{\nu} W_{\mu}^{+} \bar{t} \sigma^{\mu\nu} (\bar{f}_2^L P_L + \bar{f}_2^R P_R) b \right], \quad (4)
 \end{aligned}$$

where g is the weak coupling constant, V_{tb} is the element of the CKM matrix, m_W is the mass of the W boson, $P_{R/L} = \frac{1}{2}(1 \pm \gamma_5)$ are the chirality projectors, $\sigma^{\mu\nu} = \frac{i}{2}[\gamma^{\mu}, \gamma^{\nu}]$, f_i^L , f_i^R , \bar{f}_i^L and \bar{f}_i^R , $i = 1, 2$, are form factors which can be complex in general. The SM Wtb interaction is reproduced if $f_1^L = \bar{f}_1^L = 1$ and all the remaining form factors are set to 0.

The implementation of the right-handed vector coupling is straightforward, as it is present in the neutral current interaction SM vertices $f\bar{f}Z$ and $f\bar{f}\gamma$. However, the tensor couplings of (4) are not present in the SM and require new routines for calculating the corresponding helicity matrix ele-

ments. Therefore, a routine library `carlolib` has been supplemented with the following new subroutines: `btwan.f`, `btwmd.f`, `bwtan.f`, `bwtmd.f`, `tbwan.f`, `tbwmd.f`, `wbtan.f`, `wbtd.f`, `fefan.f`, `ffvan.f`, `fvfan.f`, `vffan.f`. They allow to calculate all the helicity amplitudes that are necessary for computing cross sections of any process involving the anomalous Wtb coupling defined by (4) and the lowest order top quark width Γ_t which enters the top quark propagator through the complex mass parameter defined in Eq. (13) of [1]. If CP is conserved then the following relationships between the form factors of (4) hold:

$$\bar{f}_1^{R*} = f_1^R, \quad \bar{f}_1^{L*} = f_1^L, \quad \bar{f}_2^{R*} = f_2^L, \quad \bar{f}_2^{L*} = f_2^R. \quad (5)$$

Γ_t is calculated anew, every time the form factors f_i^L , f_i^R , \bar{f}_i^L and \bar{f}_i^R , $i = 1, 2$, are changed. It should be stressed that for CP-odd choices of the form factors, i.e., if they do not satisfy (5), the widths Γ_t of t and $\Gamma_{\bar{t}}$ of \bar{t} differ from each other. Thus, both widths are calculated and the following rule is applied to substitute the width in the s -channel top quark propagator: Γ_t is used if the propagator goes into W^+b and $\Gamma_{\bar{t}}$ is used if the propagator goes into $W^-\bar{b}$. The rule does not work for the propagators in t - or u -channels, but the actual value of the top quark width should not play much of a role in them.

A new version of `carlomat` allows to make predictions for the top quark production and decay in hadronic collisions, through different underlying partonic processes, while taking into account complete sets of the lowest order Feynman diagrams and full information on spin correlations between the top quark and its decay products. It was used to obtain theoretical predictions in the presence of anomalous Wtb coupling for the forward-backward asymmetry in top quark pair production at the Tevatron [5] and for distributions of μ^- in the top quark pair production reaction $pp \rightarrow bu\bar{d}\bar{b}\mu^-\bar{\nu}_\mu$ at the LHC [6]. It can also be applied for studying anomalous effects in the top quark production and decay in e^+e^- collisions at a linear collider [7], [8], as it was done before with ‘‘hand made’’ modifications of a program `eett6f` [9].

2.6 Anomalous top–higgs Yukawa coupling

Due to the large top quark mass, the top–higgs Yukawa coupling

$$g_{t\bar{t}h} = m_t/v, \quad \text{with} \quad v = (\sqrt{2}G_F)^{-1/2} \simeq 246 \text{ GeV}, \quad (6)$$

is by far the biggest Yukawa coupling of SM. Its measurement, which may bring hints towards better understanding of the electroweak (EW) symmetry breaking mechanism of the SM, will certainly be one of the key points in the study of a profile of recently discovered candidate for the higgs boson [10].

The most general Lagrangian of $t\bar{t}h$ interaction including corrections from dimension-six operators that has been implemented in the program has the following form [11]

$$\mathcal{L}_{t\bar{t}h} = g_{t\bar{t}h} \bar{t} (f + if'\gamma_5) th, \quad (7)$$

where f and f' that describe the scalar and pseudoscalar departures, respectively, from a purely scalar top–higgs Yukawa coupling $g_{t\bar{t}h}$ of SM are assumed to be real. The top–higgs Yukawa coupling of SM is reproduced in Eq. (7) for $f = 1$ and $f' = 0$.

Implementation of the general coupling of Eq. (7) in the program was relatively easy, as in the complex mass scheme [12], the coupling $g_{t\bar{t}h}$ is of the complex type. It is parametrized of `carlomat` in the following way:

$$g_{t\bar{t}h} = -e_W \frac{M_t}{2 \sin \theta_W M_W}, \quad (8)$$

where complex masses M_t and M_W are defined in Eq. (13) of [1], and the complex EW mixing parameter $\sin \theta_W$ is defined in Eq. (14) of [1]. The electric charge e_W of Eq. (8) that enters multiplicatively all the EW couplings can be defined as either a real or complex quantity, by selecting an appropriate value of a flag `ialpha` in `carlocom.f`.

If we now write Lagrangian (7) in the form

$$\mathcal{L}_{t\bar{t}h} = \bar{t} \left(f_{t\bar{t}h}^{(R)} P_R + f_{t\bar{t}h}^{(L)} P_L \right) t h \quad (9)$$

and take into account the form of the γ_5 and $P_{R/L} = \frac{1}{2}(1 \pm \gamma_5)$ matrices in the Weyl representation:

$$\gamma_5 = \begin{pmatrix} -\mathbb{I} & 0 \\ 0 & \mathbb{I} \end{pmatrix}, \quad P_R = \begin{pmatrix} 0 & 0 \\ 0 & \mathbb{I} \end{pmatrix}, \quad P_L = \begin{pmatrix} -\mathbb{I} & 0 \\ 0 & 0 \end{pmatrix}, \quad (10)$$

where \mathbb{I} is a 2×2 unit matrix, then we will immediately see that

$$f_{t\bar{t}h}^{(R)} = g_{t\bar{t}h} (f + i f'), \quad f_{t\bar{t}h}^{(L)} = g_{t\bar{t}h} (f - i f'). \quad (11)$$

As the SM Lagrangian of the top–higgs Yukawa interaction in `carlomat` has the same form as Lagrangian (9) with $f_{t\bar{t}h}^{(R)} = f_{t\bar{t}h}^{(L)} = g_{t\bar{t}h}$, substitutions (11) are practically the only change that is required in the program.

The current version of `carlomat` was used in [13] to study effects of the anomalous $t\bar{t}h$ coupling of Eq. (7) on the differential distributions in rapidity and angles of the μ^- in the reaction $pp \rightarrow b u \bar{d} \bar{b} \mu^- \bar{\nu}_\mu b \bar{b}$ which is one of the channels of associated production of the top quark pair and higgs boson in proton–proton collisions at the LHC. The dominant contribution to the reaction comes from the underlying gluon–gluon fusion partonic process (3) examples of the Feynman diagrams of which are shown in Fig. 3, where the coupling corresponding to Lagrangian (7) has been indicated with a blob.

2.7 Scalar electrodynamics

The knowledge of energy dependence of the total cross section of electron-positron annihilation into hadrons $\sigma_{e^+e^- \rightarrow \text{hadrons}}(s)$ allows, through dispersion relations, for determination of hadronic contributions to the vacuum polarization, which in turn are necessary for improving precision of theoretical predictions for the muon anomalous magnetic moment and play an important role in the evolution of the fine structure constant from the Thomson limit to high energy scales. Theoretical predictions for $\sigma_{e^+e^- \rightarrow \text{hadrons}}(s)$ within quantum chromodynamics are possible only in the perturbative regime of the theory, i.e. in the high energy range, where due to the asymptotic freedom,

the strong coupling constant is small. In the energy range below the J/ψ threshold, $\sigma_{e^+e^- \rightarrow \text{hadrons}}(s)$ must be measured, either by the initial beam energy scan, or with the use of a radiative return method [14]. The idea behind the method is that the actual energy of e^+e^- scattering in the radiative reaction $e^+e^- \rightarrow \text{hadrons} + \gamma$ becomes smaller if a hard photon is emitted off the initial electron or positron prior to their annihilation. Thus, if the hard photon energy is measured and the photon emission off the final state hadrons is properly modelled, it is possible to determine the cross section of $e^+e^- \rightarrow \text{hadrons}$ at the reduced energy from the corresponding radiative process being measured at a fixed energy in the centre of mass system. At low energies, such radiative hadronic final states consist mostly of pions, accompanied by one or more photons.

The scalar quantum electrodynamics (sQED) is a theoretical framework that allows to describe effectively the low energetic electromagnetic interaction of charged pions. Despite being bound states of the electrically charged quarks, at low energies, π^\pm can be treated as pointlike particles and represented by a complex scalar field ϕ . The $U(1)$ gauge invariant Lagrangian of sQED that is implemented in `carlomat` has the following form:

$$\mathcal{L}_\pi^{\text{sQED}} = \partial_\mu \phi (\partial^\mu \phi)^* - m_\pi^2 \phi \phi^* - ie (\phi^* \partial_\mu \phi - \phi \partial_\mu \phi^*) A^\mu + e^2 g_{\mu\nu} \phi \phi^* A^\mu A^\nu. \quad (12)$$

The corresponding Feynman rules can be found, e.g., in [15]. The bound state nature of the charged pion is taken into account by the substitutions:

$$e \rightarrow eF_\pi(q^2), \quad e^2 \rightarrow e^2 |F_\pi(q^2)|^2,$$

where $F_\pi(q^2)$ is the charged pion form factor [15]. The latter has not yet been implemented in the program.

3 Other changes and preparation for running

Other minor changes to the program, including corrections of a few bugs are described in the readme file. `carlomat` v. 2.0 is distributed as a single `tar.gz` archive `carlomat_2.0.tgz`. After executing a command

```
tar -xzvf carlomat_2.0.tgz
a directory carlomat_2.0 will be created.
```

In order to prepare the program for running, the user should follow the following steps:

- select a Fortran 90 compiler in `makefile`'s of `code_generation` and `mc_computation` and compile all the routines stored in `carllib` with the same compiler;
- go to `code_generation`, specify the process and available options in `carlomat.f` and execute `make code` from the command line.

Once the code generation is finished, the color matrix is compiled and computed. The control output file `test` in `code_generation` should reproduce the delivered file `test0`.

When the code generation is accomplished:

- go to `mc_computation`, choose the required options and the centre of mass energy by editing properly `carlocom.f` and execute `make mc` in the command line.

Note, that whenever the Fortran compiler in `mc_computation` is changed, or a compiled program is transferred from a machine with different architecture, then all the object and module files in the directory should be deleted by executing the commands:

```
rm *.o
rm *.mod
```

and all the files in `carllib` should be compiled anew.

After finishing the run all output files are automatically copied to `test_output`. They should reproduce the files delivered in `test_output0`. The basic output of the MC run is stored in a file whose name starts with `tot`. Files `db...` and `d1...` contain data for making plots of differential cross sections with boxes and lines, respectively, with the use of `gnuplot`. The user can define his/her own distributions by modifying appropriately a files `calcdis.f` and `distribs.f`.

Acknowledgments: This project was supported in part with financial resources of the Polish National Science Centre (NCN) under grant decision number DEC-2011/03/B/ST6/01615 and by the Research Executive Agency (REA) of the European Union under the Grant Agreement number PITN-GA-2010-264564 (LHCPhenoNet).

References

- [1] K. Kołodziej, *Comput. Phys. Commun.* **180** (2009) 1671;
K. Kołodziej, *Acta Phys. Polon.* **B42** (2011) 2477.
- [2] J. Pumplin et al., *JHEP* **07** (2002) 012.
- [3] J. Beringer et al. (Particle Data Group), *Phys. Rev.* **D86** (2012) 010001.
- [4] G.L. Kane, G.A. Ladinsky, C.-P. Yuan, *Phys. Rev.* **D45** (1992) 124.
- [5] K. Kołodziej, *Phys. Lett.* **B710** (2012), 671–675, [arXiv:1110.2103].
- [6] K. Kołodziej, arXiv:1212.6733.
- [7] James Brau, Yasuhiro Okada, Nicholas Walker, *et al.* [ILC Reference Design Report Volume 1 - Executive Summary], arXiv:0712.1950;
J.A. Aguilar-Saavedra *et al.* [ECFA/DESY LC Physics Working Group Collaboration], arXiv:hep-ph/0106315;
T. Abe *et al.*, [American Linear Collider Working Group Collaboration], arXiv:hep-ex/0106056;
K. Abe *et al.* [ACFA Linear Collider Working Group Collaboration], arXiv:hep-ph/0109166.

- [8] R.W. Assmann *et.al.* [CLIC Study Team], CERN 2000–008;
H. Braun *et. al.* [CLIC Study Group], CERN-OPEN-2008-021, CLIC-Note-764.
- [9] K. Kołodziej, Phys. Lett. **B584** (2004) 89;
K. Kołodziej, Comput. Phys. Commun. **151** (2003) 339.
- [10] ATLAS Collaboration, Phys. Lett. **B716** (2012) 1;
CMS Collaboration, Phys. Lett. **B716** (2012) 30.
- [11] J.A. Aguilar-Saavedra, Nucl. Phys. **B821** (2009) 215 [arXiv:0904.2387].
- [12] A. Denner, S. Dittmaier, M. Roth, D. Wackeroth, Nucl. Phys. B560 (1999) 33 and Comput. Phys. Commun. 153 (2003) 462.
- [13] K. Kołodziej, arXiv:1303.4962.
- [14] Min-Shih Chen and P. M. Zerwas, Phys. Rev. D 11 (1975) 58.
- [15] F. Jegerlehner, *The Anomalous Magnetic Moment of the Muon*, Springer, Nov. 2007, ISBN 9783540726333.